

5

Experience from the application of Reliability Fatigue Crack Growth Analyses on Real Life Offshore Platform: Parametric Study and Sensitivity Analysis

Alberto ABATE ^a and Massimiliano ERRIGO ^b

^a Systems and Standards Department, Agip S.p.A.
via Emilia 1, 20097 S. Donato Milanese (Milano), Italy
Structural Engineering Department, Politecnico di Milano
Piazza Leonardo da Vinci 32, 20133 Milano, Italy

^b Offshore Engineering Department, Agip S.p.A.
via Emilia 1, 20097 S. Donato Milanese (Milano), Italy

1. INTRODUCTION

In the present study a requalification scenario of an existing offshore steel jacket platform (fig.1) has been investigated (ref./1/). The requalification process of an offshore structure brings together structural and reliability analyses, inspections data interpretation and rational inspections planning over the operating life; it is a key aspect in the management of a platform for several reasons:

- many platforms have reached their design service life;
- some of them are still temporarily manned;
- structures installed before 1970 have not been designed taking into account fatigue phenomena;
- the employed reliability analyses allow explicit consideration of specific damage conditions observed through inspection;
- it is possible to optimise inspection costs, frequencies and acceptable risk level.

The main goal of this contribution is to show some practical aspects affecting the results of fatigue reliability crack growth analyses on a typical Adriatic sea platform. The focus is on the selection of the suitable characteristics of the basic variables employed in the limit state function and on parametric and sensitivity analysis. In this way it is possible to identify the main sources of uncertainties on which it would be appropriate to concentrate efforts to increase platform reliability. The fracture mechanics approach in a probabilistic formulation offers a basis to develop a rational treatment of such uncertainties.

2. LIMIT STATE FUNCTION MODELLING

The study of the fatigue problem according to the fracture mechanics approach is based on the Paris-Erdogan law (ref./2/). It relates the crack depth increment Δa , during one load cycle, to the stress intensity factor range Δk , in the same load cycle. Since the crack increment for a load cycle is generally very little if compared to the crack dimension itself, the Paris-Erdogan law can be formulated in an incremental way:

$$\frac{da}{dN} = C \cdot (\Delta k)^m \quad (1)$$

where dN is the increment of stress cycles number, whereas C and m are material constants.

The stress intensity factor range Δk is expressed by the following formulation:

$$\Delta k = \Delta\sigma \cdot Y(a) \cdot \sqrt{\pi \cdot a} \quad (2)$$

where $\Delta\sigma$ is the far-field stress range, whereas $Y(a)$ is the geometry function and depends on the crack depth a .

The failure criteria is based on the fact that the crack depth a_T , propagated in the time range $(T - T_0)$, exceeds the critical crack dimension a_C , assumed to be equal to the element thickness. This criteria can be formulated as follows:

$$a_C - a_T \leq 0 \quad (3)$$

Introducing the functions $R(a)$, "structural resistance", and $L(T)$, "load term", and applying the failure criteria of equation (3), the safety margin can be defined as follows (ref./3/):

$$M = R(a) - L(T) \quad (4)$$

$$M = \int_{a_0}^{a_C} \frac{da}{Y(a)^m \cdot (\sqrt{\pi \cdot a})^m} - \exp(\ln C) \cdot \frac{T - T_0}{20} \cdot \sum_{i=1}^4 N_i \cdot A_i^m \cdot \Gamma\left(1 + \frac{m}{B_i}\right) = 0 \quad (5)$$

In the above equation, the contribution of four wave direction has been considered in the load term.

3. RELIABILITY UPDATING BASED ON INSPECTION RESULTS

Platforms in service are inspected to detect cracks before they become critical. A crack can be found at the time T_i and its length measured:

$$a(T_i) = a_{mi} \quad (6)$$

where a_{mi} is generally random due to measurement uncertainties. Then the safety margin can be defined as:

$$M_i = \int_{a_0}^{a_{mi}} \frac{da}{Y(a)^m \cdot (\sqrt{\pi \cdot a})^m} - \exp(\ln C) \cdot \frac{T - T_0}{20} \cdot \sum_{i=1}^4 N_i \cdot A_i^m \cdot \Gamma\left(1 + \frac{m}{B_i}\right) = 0 \quad (7)$$

A second type of inspection result is that no crack is detected, thus:

$$a(T_i) \leq a_d \quad (8)$$

where a_d is the smallest detectable crack length, depending on the inspection method used.

Similarly:

$$M = \int_{a_0}^{a_d} \frac{da}{Y(a)^m \cdot (\sqrt{\pi \cdot a})^m} - \exp(\ln C) \cdot \frac{T - T_0}{20} \cdot \sum_{i=1}^4 N_i \cdot A_i^m \cdot \Gamma\left(1 + \frac{m}{B_i}\right) \geq 0 \quad (9)$$

4. VARIABLES MODELLING

In the limit state equation (5) the employed variables can be modelled as random or deterministic. The considered model for each of them are reported below and summarised in table 1.

4.1. Initial micro-crack a_0

The variable a_0 has been assumed to be exponentially distributed and its cumulative distribution function has the following expression, ref /4/ and /5/:

$$F_{A_0}(a_0) = 1 - \exp[-\lambda \cdot (a_0 - \bar{a})] \quad (10)$$

in which a mean value of 0.11 mm has been considered.

4.2. Critical crack depth a_C and thickness t

The Gaussian stochastic model for both the variables a_C and t has been assumed. The inspection results carried out on the platform, have been used to estimate mean value and standard deviation of these variables.

4.3. Initial time T_0 and final time T

The variables T_0 and T are deterministic; in a conservative way it has been considered $T_0=0$, that means to have the crack beginning when the platform was installed (1971). The T value depends on the date on which it is desired to have the reliability results during the parametric study execution.

4.4. Wave numbers N

In equation (5) N_i represents the wave number occurring in the i direction expected in the time range $(T - T_0)$; it is considered a deterministic variable.

4.5. Material constants C and m

In order to model the material constants, the results of several studies reported in ref./4/, /6/, /7/ and /8/, have been used. In the mentioned references it seems to be accepted the use of normal distribution for both the variables $\ln C$ and m , with the mean values equal to -29.75 and 3.0 respectively, and the corresponding variances 0.5 and 0.09. The numerous experimental data have proved a correlation coefficient ρ equal to -0.9.

4.6. Weibull distribution parameters A and B

To solve equation (5) it is necessary to determine the values of the two Weibull scale and shape parameters A and B that define the cumulative distribution function of the stress range S . It has the following formulation:

$$F_S(S) = 1 - \exp\left[-\left(\frac{S}{A}\right)^B\right] \quad (11)$$

Instead of averaging the effects of the four wave directions considered to obtain only one curve as usually done, four "long term stress range distribution" curves per analysed connection have been considered; each i curve represents the probability that a S value is exceeded for that i wave direction.

In ref./4/, /6/, /7/ and /8/ it is described a suitable stochastic representation of the scale and shape parameters of the Weibull distribution: for the parameters A_i , a lognormal distribution has been assumed and a coefficient of variation equal to 10% has been considered; similarly, for the parameters B_i a lognormal distribution has been used. This choice is justified by the observation that, since B ranges between 0.4 and 0.7 for the Adriatic Sea, using the lognormal distribution it is taken into account that B can not physically assume negative values. A COV of 10% has been used.

4.7. Geometry function $Y(a)$

The geometry function $Y(a)$ formulation has been extracted from ref./6/, confirmed also by ref./4/ due to its suitable adhesion to the problem physics reality:

$$Y_{\text{eff,average}}(a) = Y_{\text{unw}}(a) \cdot M_k(a) \quad (12)$$

where Y_{unw} represents the geometry function that takes into account the assumed semi-elliptical shape of the crack, neglecting the welding effect ("unwelded"), while $M_k(a)$ is a correction factor that considers the influence of the welding in the stress concentration estimate. They have the following expressions, ref./9/ and /10/:

$$Y_{\text{unw}}(a) = \left[1.08 - 0.7 \cdot \left(\frac{a}{t} \right) \right] \quad (13)$$

$$M_k(a) = 1.0 + 1.24 \cdot \exp\left[-22.1 \cdot \left(\frac{a}{t}\right)\right] - 3.17 \cdot \exp\left[-357 \cdot \left(\frac{a}{t}\right)\right] \quad (14)$$

To consider the uncertainty related to the above formulation of the $Y_{\text{eff,average}}(a)$, a stochastic variable Y_1 has been introduced (ref./8/). Therefore, the final modelling of the geometry function $Y(a)$ is the following:

$$Y(a) = Y_1 \cdot Y_{\text{eff,average}}(a) \quad (15)$$

Concerning Y_1 a lognormal distribution with unitary mean value and COV equal to 0.1 has been adopted.

4.8 Minimum detectable crack depth a_d

The subsea inspections can not cover all the joints of the platform. Furthermore, due to the uncertainty within the adopted inspection method, a probability exists that, at the time of the inspection T_i , a crack of length $2c$ (or depth a) is not detected.

Therefore, the Probability Of Detection curve, POD, assumes a considerable importance

and it is obviously a function of the adopted detection method. The inspections are mainly performed using the "Magnetic Particle Inspection" (MPI). Due to the good accuracy of the execution of the inspections, it is possible to use the POD curve proposed by a Brite study mentioned in ref./8/, in which the cumulative distribution function of the crack detection has the following expression:

$$\text{POD}(2c) = P_0 \cdot \{1 - \exp[-\beta \cdot (2c - a)]\} \quad (16)$$

where the POD curve is a function of the superficial crack length $2c$, P_0 has a value very close to unity and represents the probability of detection of a long crack, β is the growing speed of the curve, 0.04 mm^{-1} (ref./8/), while a is the minimum detectable crack length, 6.67 mm (ref./11/). A comparison with different formulations from ref. /7/ and /8/ has been made, in which there is the same hypothesis $\frac{a}{2c}$ as constant ratio (semi-elliptical shape crack).

Taking into account some experimental results of offshore tubular joints (ref./8/), it has been possible to assess a more appropriate formulation of the POD curve in which the ratio $\frac{a}{c}$ is deeply conditioned by the relative crack depth $\frac{a}{t}$, see figure 2; in particular, $\frac{a}{c}$ decreases when the ratio $\frac{a}{t}$ grows. Analysing these experimental results, it can be noted that in the initial phase, the crack has nearly a circular shape and only during its development becomes elliptical.

The POD curve proposed in this study is shown in figure 3 together with the other formulations.

5. ANALYSIS OF RESULTS

A summary of the reliability fatigue analysis results and their discussion and interpretation are in the following. It must be pointed out that the reliability index β has been calculated using the second order approximation method (SORM).

In figure 4 the β index behaviour for a K joint is shown. The values have been calculated by the program PROBAN (PROBabilistic ANalysis, Det Norske Veritas Sesam) every six months. Analysing the results, it can be noted that after a few years of service β is below the range of the allowable values. These last ones have been evaluated in accordance with ref./11/, in the case of manned platform (lower line) or not one (upper line).

From these figures it stands out the big increment of the β index after the inspection performed in 1987. This increment, due to the absence of cracks, keeps the values of β above the limit even after the second considered inspection in 1991. It is evident that using the fracture mechanics approach in the reliability fatigue analysis it is possible to get an increment of the safety of the structure due to the possibility to take into consideration added information on the structure state as the time varying.

Figure 5 shows graphically the importance factors of all the variables after 22 years of service. Also the relative importance factors of the B_i parameters has been calculated in order to investigate the relative influence of the single wave direction in the considered joints (fig.6). After this evidence, it is possible to consider that, due to the different location that each joint has in the structure, it is reasonably important to consider separately the single wave direction

contributes in the limit state function.

A sensitivity analysis to study the effects of the parameters on the β index, has been developed. A new reliability analysis has been performed every modification of the values of the random variables (considered as the parameter to be changed). Table 2 summarises the different variations in the sensitivity analysis carried out.

Examining figure 7, relevant to a very critical joint, it is evident that the random variables Y_1 , $\ln C$ (together with m), a_C and t are of very low importance for the original reliability index behaviour vs time. On the opposite, it is more evident the behaviour difference in the case where the parameters A_i and B_i COV have been changed, as shown in figure 8.

Therefore, for a periodic structure monitoring, the determination of these two measures can be very useful for a qualitative assessment of the next inspection survey.

Moreover, due to the possibility, allowed by this analysis methodology, to take into account the information coming from the inspection survey, the structure service life can be extended significantly; furthermore in order to design an inspection planning, the results of this contribution have shown, if no cracks are found, the real possibility to inspect with reasonably increased time ranges and consequently to get inspection costs reduced up to 35 %.

REFERENCES

- /1/ A. Abate - L. Losapio (1993), "Aspetti affidabilitici in ambito offshore", Politecnico di Milano, Italy
- /2/ P. Paris - F. Erdogan (1963), "A critical analysis of crack propagation laws", J. Basic Engineering Trans. ASME
- /3/ A. Almar - Naess, ed. 1985, "Fatigue Handbook for offshore steel structures", Tapir Publishers, Trondheim, Norway
- /4/ A. Karamchadani - J.I. Dalane - P. Bjerager (1992), "Systems Reliability Approach To Fatigue of Structures", Journal of Structural Engineering, Vol. 118, No. 3, Paper n. 487, ASCE
- /5/ A.H.S. Ang - W.H. Tang (1975 - 1984), "Probability Concepts in Engineering Planning and Design", Voll. 1 e 2, John Wiley & Sons, Toronto
- /6/ F. Kirkemo (1988), "Applications of probabilistic fracture mechanics to offshore structures", Appl. Mech. Rev.
- /7/ R. Skjøng - R. Torhaug (1991), "Rational Methods for Fatigue Design and Inspection Planning of Offshore Structures", Marine Structures Vol. 4, Elsevier Science Publishers, England
- /8/ Rapporto D' Appolonia No. 89 - 302 (1990), "Analisi Probabilistica Propagazione Cricca", Vol. 1, Genova
- /9/ I.S. Raju - J.C. Newman (1981), "An Empirical stress intensity factor equation for surface crack", Engineering Fracture Mechanics
- /10/ I.J. Smith - S.J. Hurworth (1984), "The effect of geometry changes upon the predicted fatigue strength of welded joints", Res. Report 244, Welding Inst.
- /11/ Det Norske Veritas (1992), "Structural reliability analysis of Marine Structures", Classification Notes n° 30.6 DNV Classification As, Hovik, Norway

VARIABLE	MODELLING	MEAN VALUE	SCATTER
a_0	EXPONENTIAL	0.11 mm	lower bound 0.0
a_C	NORMAL	10.07 mm	COV = 0.03
T_0	DETERMINISTIC	0 anni	-
T	DETERMINISTIC	1 + 29 YEARS	-
N_1	DETERMINISTIC	38620557	-
N_2	DETERMINISTIC	36381752	-
N_3	DETERMINISTIC	42514976	-
N_4	DETERMINISTIC	36410771	-
$\ln C$	NORMAL	- 29.75	$\sigma = 0.5$
m	NORMAL	3.0	$\sigma = 0.09$
A_i	LOGNORMAL	DEPENDS ON THE CONNECTION	COV = 0.1
B_i	LOGNORMAL	DEPENDS ON THE CONNECTION	COV = 0.1
Y_1	LOGNORMAL	1.0	COV = 0.1
t	NORMAL	10.07 mm	COV = 0.03
a_d	ASSIGNED BY POINTS		

TAB. 1



FIG. 1

PARAMETER	MEAN VALUE	COV
Y_1	UNCHANGED	0.0
$\ln C - m$ (without correlation)	UNCHANGED	0.0
$a_0 - t$	UNCHANGED	0.0
$A_i - B_i$	UNCHANGED	0.075
$A_i - B_i$	UNCHANGED	0.05

TAB. 2

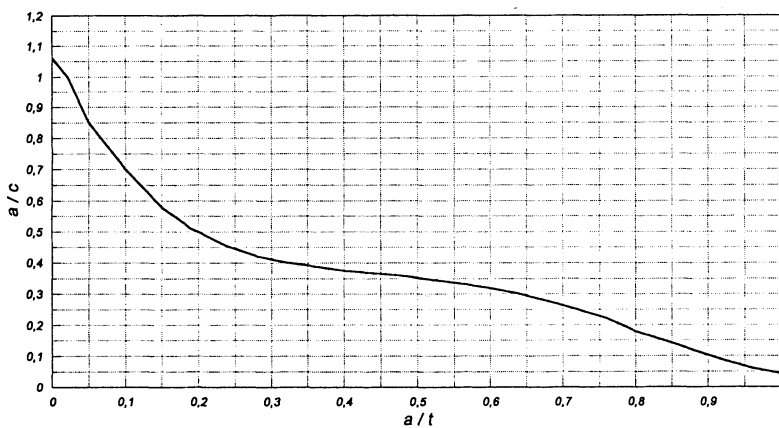


FIG. 2

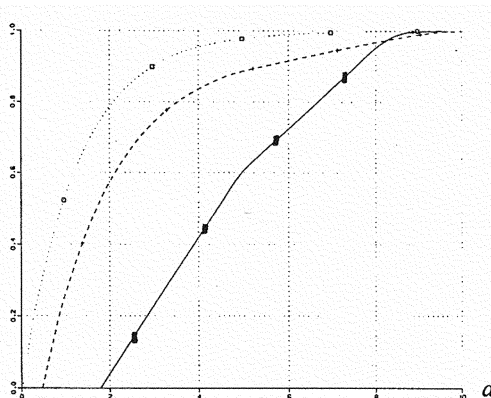


FIG. 3: ■ POD PROPOSED CURVE

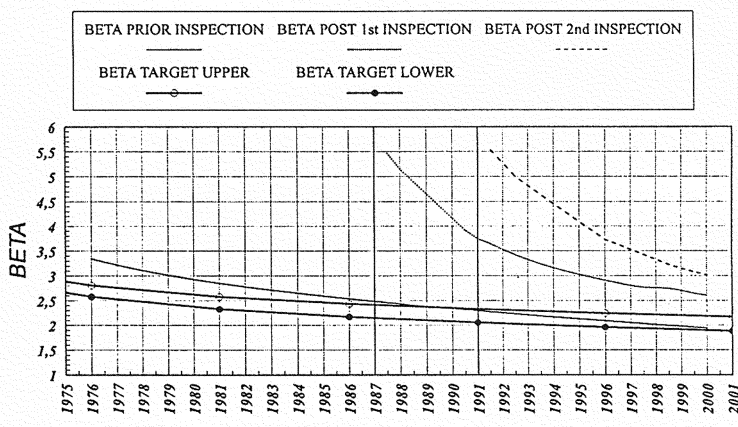


FIG. 4

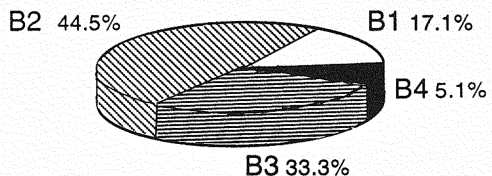
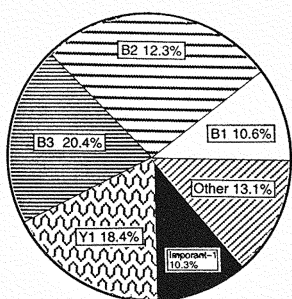


FIG. 6

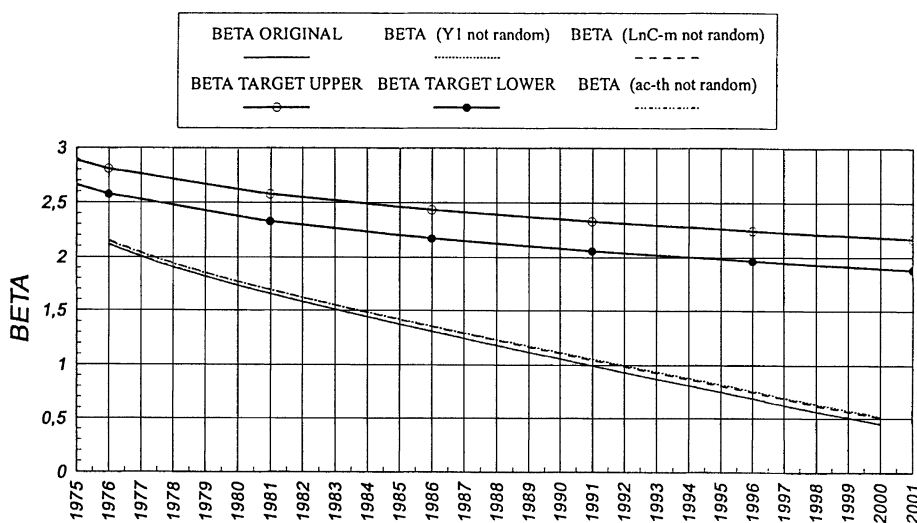


FIG. 7

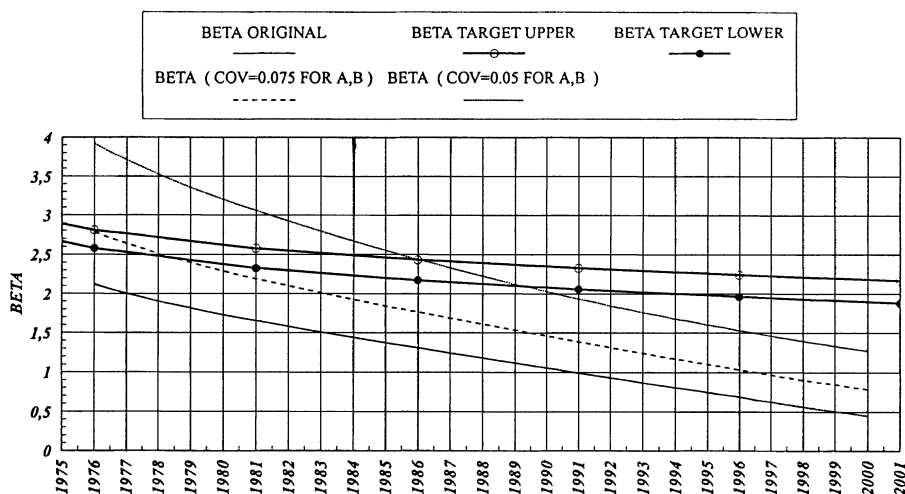


FIG. 8